

<https://doi.org/10.1038/s42003-025-08022-x>

Unveiling the early evolution of black corals



Wenjing Hao¹, Jian Han¹✉, Andrzej Baliński², Mercer R. Brugler^{3,4}, Deng Wang¹, Xin Wang⁵, Bernhard Ruthensteiner⁶, Tsuyoshi Komiya⁷, Jie Sun¹, Yuanyuan Yong¹ & Xikun Song^{1,8,9}✉

Black corals, primarily deep-sea cnidarians (Anthozoa: Antipatharia), are inferred to have originated either in the Ediacaran or Cambrian based on molecular clock estimates. However, only the fossil family Sinopathidae, comprising *Sinopathes* and *Sterictopathes*, from the Early Ordovician of Hubei, China, has been recorded in the fossil record. The affinity of this family has been questioned because of morphological inconsistencies between fossil and extant species. Here we describe two transitional species of *Sterictopathes* from the Middle Ordovician of Shaanxi, China, bridging the fossil gaps and thereby elevating the genus *Sterictopathes* to a new family, Sterictopathidae fam. nov. The hypothesized evolutionary trend toward regularity in the axial skeleton from the Ordovician to modern Antipatharia is highlighted by reduced ridges and longitudinal fusion of networks. This discovery and confirmation of Ordovician black corals paves the way for future fossil findings and offers new insights into the early evolution of Hexacorallia.

Modern antipatharians are noncalcareous, colonial anthozoans distributed in oceans worldwide ranging from shallow to hadal depths (three to 8900 meters)^{1,2}. Black corals have ecological and cultural importance³. To date, 301 extant black coral species belonging to eight families have been described⁴. Generally, it is believed that over 75% of known species occur in depths deeper than 50 m⁵. Many genera belonging to the families Antipathidae, Aphanipathidae, and Myriopathidae are reported primarily in the shallow and mesophotic depths⁶, while families like Schizopathidae and Cladopathidae are mainly distributed in the abyssal and hadal zones below 3500 m⁷. Black corals are characterized by a spiny, proteinaceous chitin-based skeleton comprised of multiple concentric layers surrounding a small central canal⁸. The skeletal spines can be triangular, conical, hooked, hemispherical, or blade-like; sometimes they are laterally compressed; they can be smooth or bearing protuberances or tubercles, with or without apical bifurcations or multi-lobed; they can be irregularly arranged or aligned in distinct longitudinal rows⁹.

Fossil records of black corals are quite sparse compared with those of calcareous corals^{10–15}. Historically, the first fossil “black coral” *Antipathes vetusta* Michelotti, 1839¹⁶ was described based on stem fragment fossils from the Miocene of Turin, Italy¹³. It has since been re-identified as a

gorgonian^{17–19}. Another Miocene fossil record of the extant species *Leopathes glaberrima* appeared in several fossil black coral lists^{10,14,15,20} but could not be traced to any morphological illustrations or descriptions.

At present, only one black coral fossil family, the Sinopathidae, composed of three species (*Sinopathes reptans*, *Sinopathes* sp., and *Sterictopathes radicans*), has been described exclusively from the same Early Ordovician Fenxiang Formation (470 Ma) in the Hubei, South China^{11,12}. The antipatharian affinity of *Sinopathes*¹¹ was contentious because of morphological differences between fossil and extant species^{10,21}. The concerns mainly focused on the morphology of the spines of *Sinopathes reptans*, which are sculptured with distinct and continuous longitudinal costellae, as well as the presence of some tubular spines with a central canal¹⁰. This is inconsistent with the morphology of modern black corals. Brugler et al.¹⁰ even hypothesized *Sinopathes reptans* as a cnidarian closely related to the hydrozoan *Hydractinia*, as spine-like structures are also present in the hydrorhiza mat of some encrusting *Hydractinia* colonies²². Baliński and Sun¹² argued that *Sinopathes reptans* and *Hydractinia* differ in colonial growth patterns: the former forming upright and branched colonies, while the latter generates mat-like or stoloniferous encrusting colonies¹². Additionally, they also explained that the spines of *Sinopathes reptans* are multi-layered and solid.

¹Shaanxi Key Laboratory of Early Life and Environments (SKLELE), State Key Laboratory of Continental Evolution and Early Life (SKLCEE), Department of Geology, Northwest University, Xi'an, China. ²Institute of Paleobiology, Polish Academy of Sciences, Warszawa, Poland. ³Department of Natural Sciences, University of South Carolina Beaufort, Beaufort, SC, USA. ⁴Division of Invertebrate Zoology, American Museum of Natural History, New York, NY, USA. ⁵Centre for Orogenic Belt Geology, CGS, Xi'an Center of China Geological Survey, Xi'an, China. ⁶SNSB-Zoologische Staatssammlung München, München, Germany. ⁷Department of Earth Science and Astronomy, Graduate School of Arts and Sciences, The University of Tokyo, Tokyo, Japan. ⁸Institute of Deep-Sea Science and Engineering, Chinese Academy of Sciences, Sanya, China. ⁹State Key Laboratory of Marine Environmental Science, College of Ocean and Earth Sciences, Xiamen University, Xiamen, China. ✉e-mail: elihanj@nwu.edu.cn; xksong@idsse.ac.cn

Moreover, the exceptionally rare tubular-like spine with a central canal was attributed to a preservation artifact¹². But they did not directly address the concern on the delicate longitudinal costellae on the spines¹².

Except for the abovementioned fine costellae on the spines, the arrangement pattern of spines, a diagnosis for antipatharian systematics, also varies significantly in the Sinopathidae. Spines of most extant antipatharians are rather uniform and are arranged in longitudinal rows^{23–26}, albeit a few of species exhibit irregularly arranged spines^{27,28}. Whereas spines of *Sinopathes* are distributed irregularly and vary in size and shape^{11,12}. The affinity of *Sterictopathes* is also puzzling as its typical anastomosing networks formed by smooth spines buttressed by radiating, plate-like ridges¹² are absent in extant black corals. Because of the huge morphological differences between these fossils and extant forms, both *Sinopathes* and *Sterictopathes* were excluded from two recent time-calibrated molecular phylogenies that point to Ediacaran or Cambrian origin of Antipatharia^{29,30}.

Herein we report two intermediate species (*Sterictopathes seira* sp. nov., *Sterictopathes* sp.) based on 256 specimens from the Middle Ordovician Xiliangsi Formation of the Fanjiagou section in Shaanxi, China, providing evidence to bridge the fossil gaps between the early Ordovician genus *Sterictopathes* and extant relatives, and shedding new light on the evolution of skeleton regularity in black corals.

Results

Systematic paleontology

Phylum Cnidaria Hatschek, 1888

Sub-Phylum Anthozoa Ehrenberg, 1834

Class Hexacorallia Haeckel, 1896

Order Antipatharia Milne-Edwards & Haime, 1857

Family Sterictopathidae Hao, Han, Baliński, Brugler & Song fam. nov

LSIDurn:1sid:zoobank.org:act:8C4E500A-807D-4B40-B027-BE3DD0BBA1D

Type genus. *Sterictopathes* Baliński & Sun, 2017.

Etymology. From the type genus *Sterictopathes* Baliński & Sun, 2017.

Diagnosis. Corallum consists of an encrusted basal plate and an upright, branching stem, both covered with spines and high ridges radiating from the spine bases, usually forming an anastomosing network. Branches thin-walled. Spines cylindrical to conical, blunt, irregularly distributed, occasionally arranged in short longitudinal or oblique rows.

Remarks. Initially, family Sinopathidae included *Sinopathes*, characterized by a smooth colony surface, and *Sterictopathes*, which has a strongly sculptured surface¹². However, if taking into account the noticeable difference in their skeleton ornamentation, it seems more appropriate to erect a new family Sterictopathidae, and confine Sinopathidae to the type genus *Sinopathes*.

Genus. *Sterictopathes* Baliński & Sun, 2017

Type species. *Sterictopathes radicans* Baliński & Sun, 2017

Sterictopathes seira Hao, Han, Baliński, Brugler & Song sp. nov.

LSIDurn:1sid:zoobank.org:act:C033876B-188B-4E31-B149-9884CB29DEB7

Etymology. The Greek word *seira*, meaning for line, masculine in gender, refers to the longitudinal arrangement pattern of spines and their basal ridges.

Material, locality, and horizon. A total of 253 specimens of *Sterictopathes seira* sp. nov. were recovered (Supplementary Table 1) from the Lower part of the Ordovician Xiliangsi Formation in Fanjiagou

section, Ningqiang, Shaanxi, China (Fig. 1). These specimens show a three-dimensional preservation with slight compression, and high fragmentation suggesting potential transport by currents before burial. In addition to this black coral, the fossil assemblage indicates a mixed, allocative phase of fossil deposition. It also includes abundant specimens of the benthic trilobite *Ningjianites* sp. (Supplementary Fig. 1a, b, k), an indeterminate benthic brachiopod species (Supplementary Fig. 1c), the pelagic conodonts *Lenodus antivariabilis* and *Scolopodus striatus* (Supplementary Fig. 1m, n), and the graptolites *Undulograptus austrodentatus* (Supplementary Fig. 1i, j) and *Azygograptus suecicus* (Supplementary Fig. 1d–h, l, o).

The occurrence of *Undulograptus austrodenfatus*, an index graptolite for the Darriwilian stage of the Middle Ordovician³¹, dated to approximately 467 million years ago, confirms the co-occurrence of this species with the Xiliangsi Formation in Shaanxi. This correlation is crucial to understanding the geological context of black coral occurrence. According to Lai et al.³², the Xiliangsi Formation was deposited in a nearshore shallow marine environment characterized by good light transmittance and high oxygen content. The depositional environment resembled that of the Early Ordovician Fenxiang Formation^{33,34}.

Type material. Holotype, ELI-FJG01001 (Fig. 2h); paratypes, ELI-FJG03118, ELI-FJG03595, ELI-FJG03113 (Fig. 2g, i, j).

Diagnosis. Corallum with a branching angle of about 45°. The surface of branches with spines, ridges radiating from the spine bases, and networks of ridges forming frequent deep cavities bordered by 4–17 ridges. Spines narrowly conical to cylindrical, occasionally bifid or trifid, smooth-surfaced, arranged irregularly but tending to form rows.

Description and comparisons. The studied material of *Sterictopathes seira* sp. nov. consists of fragmented coralla, mainly branches, characterized by a dense coverage of spines, ridges and network of ridges (Fig. 2g–j and Supplementary Fig. 2). Branches approximately 0.07–0.34 mm in diameter, are mostly straight or, exceptionally rarely, slightly curved (Fig. 2j and Supplementary Fig. 2c). Notably, some specimens exhibit branching at an angle of approximately 45°, with short, bramble-like second-order structures oriented parallel or perpendicular to the plane of the first-order branches (Fig. 2g).

There are multiple networks of different sizes on the surface of the branches, and polygonal networks each variably consisted of 4–13 spines connected by 2–4 sub-transverse or oblique ridges, and 2–13 sub-longitudinal ridges with thickness ranging from 1.4 to 2.9 µm (Fig. 2l). The networks are deeply concaved and smooth surfaced, depending on the number of ridges. Larger networks with more longitudinal ridges, superficially long quadrilateral, extend longitudinally (Fig. 2h).

The spines on branches are smooth-surfaced, and narrowly conical to cylindrical (Fig. 2k–n). Some of the spines are bifid or trifid (Fig. 3), and the cross section of spines exhibits circular or sub-elliptic concentric layered rings (Fig. 3). The base of the spines has 2–5 ridges, but mostly 2–3. The bases of adjacent spines are completely connected by a long, prominent, complete ridge or a short, low, much narrow incomplete one (Fig. 2m). The complete ridges are gentle hill-like in cross section, symmetrical in two ends, whereas the incomplete ones (inconspicuous ridges connecting a single spine) decrease in height and disappear distally. In addition to many oblique or sub-transverse ridges, adjacent joined ridges often form a multiple of longitudinal, subparallel zigzag rows of ridges (Fig. 4a–f).

The skeletal surface of *S. seira*, particularly in pits or in proximity to the spine base, often exhibits shallow polygonal imprints measuring 9–14 µm in diameter (Supplementary Fig. 3). Similar structures in *S. radicans* have previously been interpreted as being the imprints of secretory epithelial cells¹¹.

Micro-CT observations of virtual cross-sections of *S. seira* branches reveal a characteristic antipatharian pattern³⁵, characterized by a central canal surrounded by a multi-layered concentric structure (Fig. 5a, b, d, e).

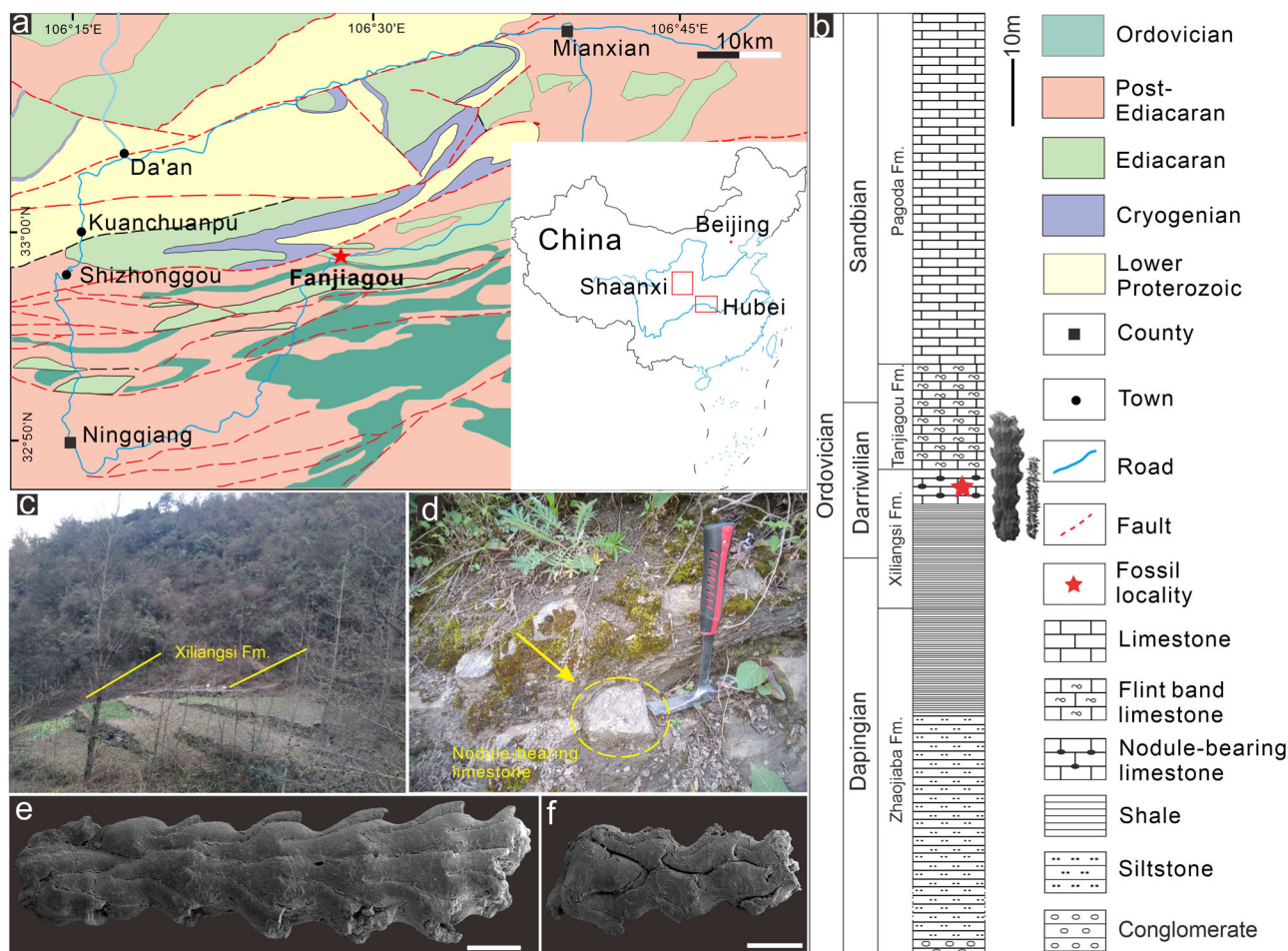


Fig. 1 | Locality and stratigraphy of the investigated Xiliangsi Formation, Fanjiagou section, Middle Ordovician, Shaanxi, China. **a** Geological maps showing the investigated Fanjiagou locality, the lower right thumbnail is adopted from a standard map of China (GS-2016-1549, Ministry of Natural Resources of China). **b** Stratigraphic column of the Xiliangsi Formation, Fanjiagou section. **c**, **d** Field

images of the Fanjiagou section bearing nodule limestones (the yellow arrow in **d**) where the investigated black coral fossils of *Sterictopathes seira* sp. nov. were recovered. The index graptolite *Unduloraptus austrodentatus* indicating the bottom of the Darriwilian Stage, ELI-FJG01320 (**e**) ELI-FJG01285 (**f**). Scale bars: **e**, **f** = 500 μ m.

Some branches reveal *Sterictopathes seira* (Fig. 5m–o) and *Sterictopathes* sp. (Fig. 5g–i) encrusting around the *Sphenothallus* tube^{12,36}, which is characterized by longitudinal, radial, thin septa-like structures (up to nine) in cross section.

Chemical component. Spectral examination reveals notable D-band (disordered organic matter) and G-band (graphitic organic matter) signatures, confirming the identification of materials as organic carbon (Supplementary Fig. 4). Additionally, Energy Dispersive X-ray spectroscopy (EDS) mapping demonstrates the relative abundance of C, with minor amounts of P and Ca (Supplementary Fig. 4), originating from secondary phosphatation, as frequently observed in Cambrian small shelly fossils³⁷. No instances of calcite or aragonite pseudocrystals replaced by apatite were detected in SEM.

Remarks. The skeletons of both *Sterictopathes seira* sp. nov. and *S. radicans* are characterized by the presence of sculpture in the form of a high, anastomosing network of ridges and spines, as well as a multi-layered, concentric structure (Fig. 2n, f and Supplementary Fig. 5p). They do, however, differ in several characters: (1) *S. seira* has larger, deeply concave cavities (approximately 139–689 μ m long and 102–120 μ m wide), delimited by 4–17 adjacent sub-longitudinal, oblique, and sub-transverse ridges and spines (Figs. 2l, 4), while *S. radicans* has smaller, flat-bottomed cavities (124–254 μ m in length and 85–128 μ m in width)

bordered by 3–4 irregularly arranged ridges (Fig. 2a–e); (2) *S. seira* exhibits multiple longitudinal rows of ridges parallel to each other (Fig. 4), while *S. radicans* exhibits randomly oriented ridges (Supplementary Fig. 5); (3) spines of *S. seira* are buttressed by straight ridges (Figs. 2m, 4), while in *S. radicans* there is occasionally no spine development at the junction of three ridges (Supplementary Fig. 5a–c); and (4) the spines of *S. seira* are mostly supported by 2–3 ridges (Fig. 2k–m), whereas those in *S. radicans* are often supported by 3–4 ridges (Fig. 2c–e).

In the present Middle Ordovician black coral collection from the Xiliangsi Formation, three rare specimens have been provisionally identified as an undetermined species within the genus *Sterictopathes*, here referred to as *Sterictopathes* sp. (Fig. 2o–t). It apparently belongs to *Sterictopathes*, as the presence of networks of ridges. The simplified spine-ridge junctions and isolated spines in *Sterictopathes* sp. quite resemble those of extant antipatharians (Fig. 5c, f; Supplementary Table 2). Meanwhile, it differs from the remaining congeneric species in several characteristics: the cavities of networks are flat-bottomed and formed by 4–12 longitudinally arranged spines and shallow ridges (in lateral view); the spines are short and conical, buttressed mostly by 0–2 straight ridges (Fig. 2o–t); adjacent ridges joined together and arranged longitudinally or slightly obliquely (Fig. 2o–t).

Phylogeny. The topology of the phylogenetic tree built using four concatenated DNA barcoding genes (Supplementary Fig. 6b) is consistent

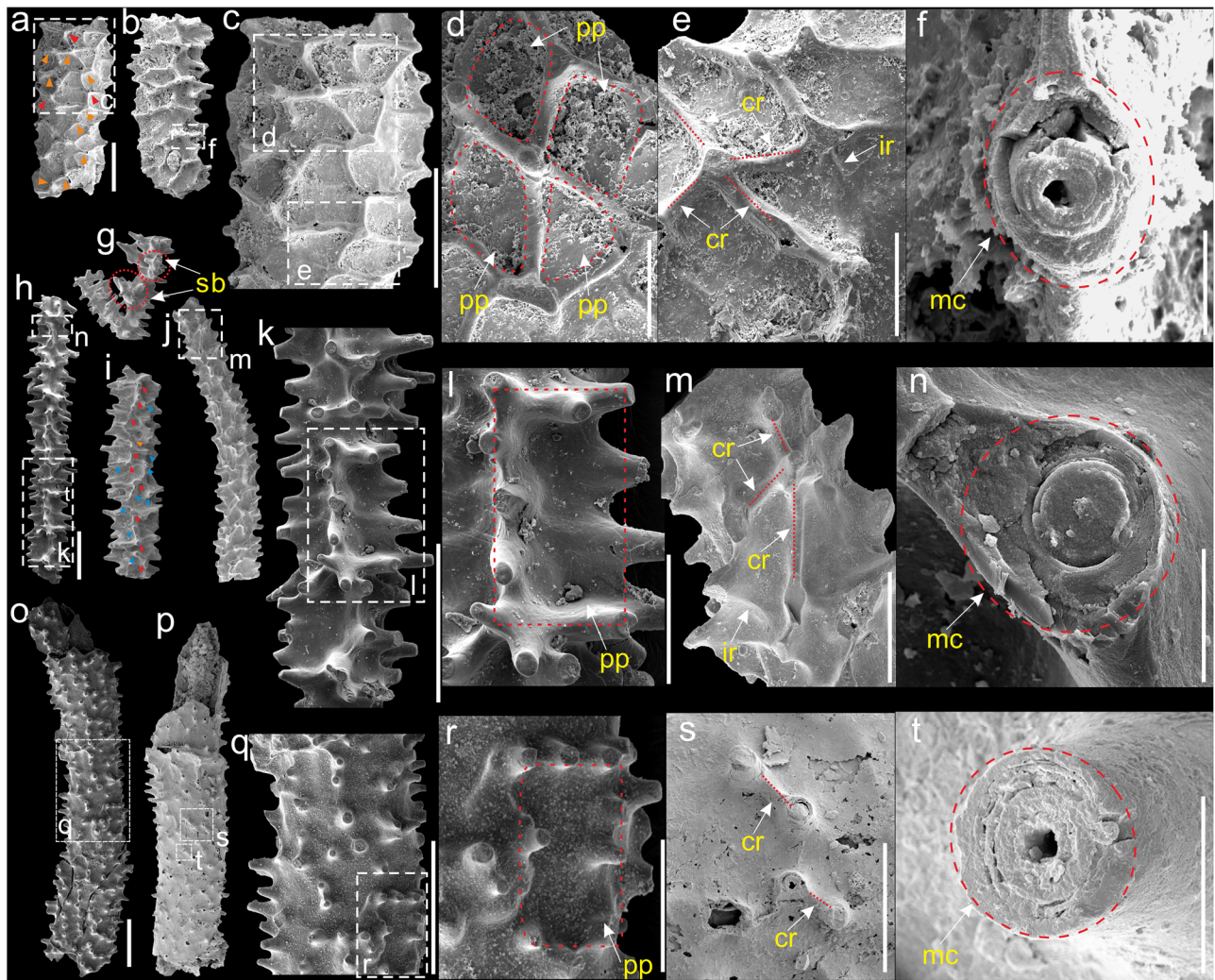


Fig. 2 | Colonies of three Ordovician black coral species of the Sterictopathidae fam. nov. **a–f** *Sterictopathes radicans* Baliński & Sun, 2017, Early Ordovician, Fenxiang Formation, Huanghua quarry, Hubei, China. **g–n** *Sterictopathes seira* sp. nov., Middle Ordovician, Xiliangsi Formations, Fanjiagou section, Ningqiang, Shaanxi, China. **o–t** *Sterictopathes* sp., Middle Ordovician, Xiliangsi Formations, Fanjiagou section, Ningqiang, Shaanxi, China. **d, l, r** Networks formed by complete and incomplete ridges. **e, m, s** Complete and incomplete ridges. **f, n, t** Multi-layered concentric structure of broken tips of branches. The arrows in (**a, i**) indicate

junctions comprised by two (blue arrows), three (red arrows), or four (orange arrows) ridges that assembled at the base of different spines, respectively. CR, complete ridge; IR incomplete ridge; MC multi-layered concentric structure; PP polyp pit; sb secondary branch, SP spine. Specimens: **a, c–e** ELI-HHC017, **b, f** ELI-HHC051, **g** ELI-FJG03118, **h, k, l, n** ELI-FJG01001 (holotype), **i** ELI-FJG03595, **j, m** ELI-FJG03113, **o, q, r** ELI-FJG02426. **p, s, t** ELI-FJG04013. Scale bars: **a–c, h–k, o–q** = 500 µm; **d, e, l, m, r, s** = 200 µm; **f, n, t** = 30 µm.

with a recent mitochondrial genomic tree or phylogenomic trees composed of fewer black coral species^{9,38}, supporting the separation of the seven extant black coral families with available barcoding data. On the morphological tree (Supplementary Fig. 6a), the fossil families Sterictopathidae and updated Sinopathidae (excluding *Sterictopathes*) form two separate monophyletic clades with Bayesian posterior probabilities (BPP) of 1.00 and 0.27, respectively. Furthermore, Sterictopathidae clusters with the paraphyletic clade of Leiopathidae, supported by a BPP value of 0.33. In the consensus tree integrating morphological and molecular data (Supplementary Fig. 6c), the family Sterictopathidae also constitutes a stable monophyletic clade (BPP value, 0.76) of Antipatharia. However, family Sinopathidae appears as a paraphyletic outgroup of extant black corals, probably due to the inclusion of unidentified *Sinopathes* specimens (*Sinopathes* sp., specimen Tianjialing T13; *Sinopathes* sp., specimen Gudongkou 115E)¹². In summary, both the morphological and the consensus trees of cladistic analysis support the monophyletic clade of Sterictopathidae as a part of Antipatharia (Fig. 6a and Supplementary Fig. 6c).

Discussion

Black coral affinities

Both Sterictopathidae and Sinopathidae possess skeletal spines and multi-layered concentric structures comparable to extant black corals. The discovery of two intermediate species (*Sterictopathes seira* and *Sterictopathes* sp.) provides key evidence to bridge fossil gaps, in particular, between the Early Ordovician *Sterictopathes reptans* and extant species, supporting the antipatharian affinities of Sterictopathidae. The fully developed (*Sterictopathes radicans*), simplified (*S. seira*), and reduced (*Sterictopathes* sp.) spiny networks represent morphological variations due to the disappearing tendency of the transversal spine-ridge junctions in Sterictopathidae (Fig. 6). Moreover, except for few partial transversal spines and ridges, the characteristic that one longitudinal ridge connecting one or two adjacent spines seen in *Sterictopathes* sp. closely resemble some of extant species (Supplementary Table 2). Notably, incomplete or complete longitudinal ridges are also present in five extant black coral families, including Leiopathidae, Antipathidae, Cladopathidae, Aphanipathidae, and Schizopathidae (Supplementary

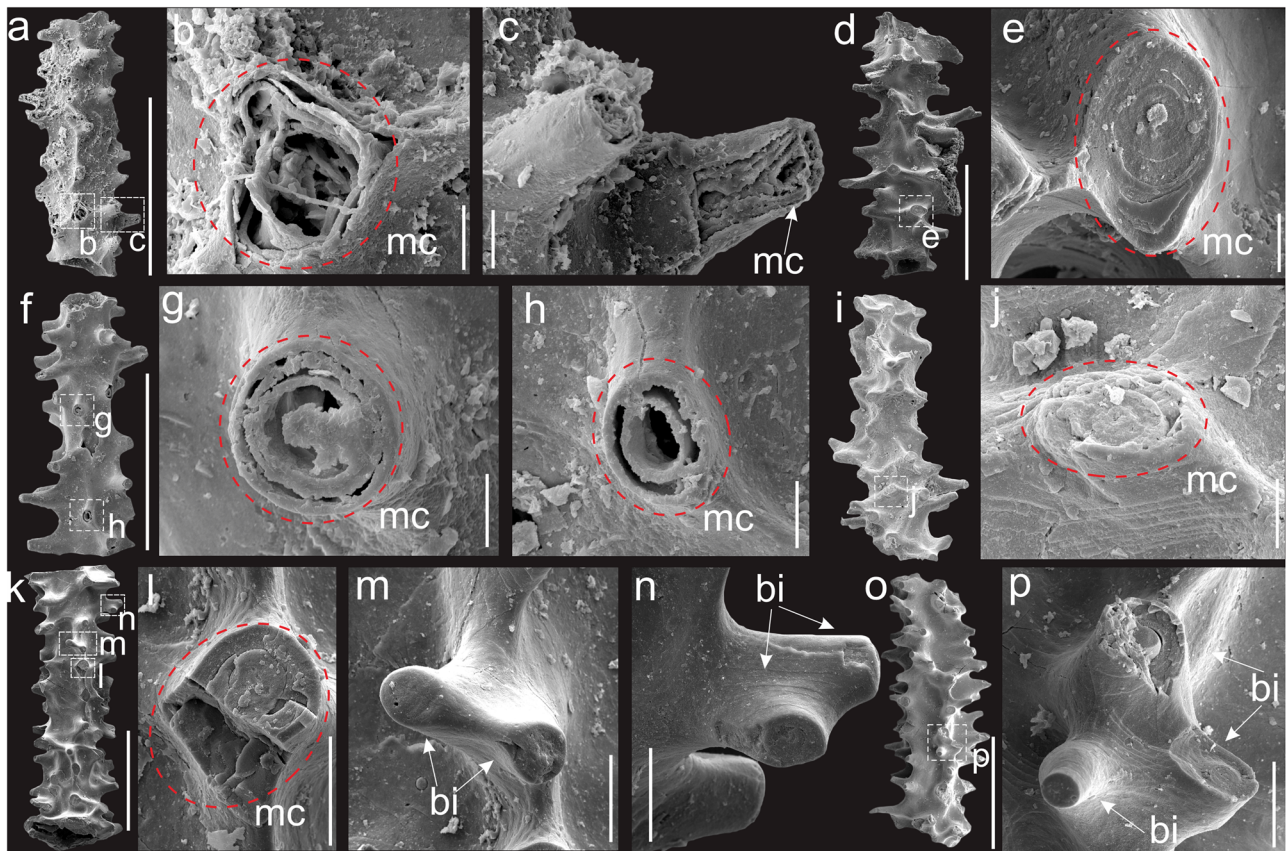


Fig. 3 | Spines of *Sterictopathes seira* sp. nov. **a–l** multi-layered concentric structure of spines. **m–p** distal bifurcation of spines. Abbreviations: BI bifurcation, MC multi-layered concentric structure. Specimens: **a–c** ELI-FJG03291, **d, e** ELI-FJG01257,

f–h ELI-FJG03149, **i, j** ELI-FJG05092, **k–n** ELI-FJG01051, **o, p** ELI-FJG02201. Scale bars: **a, d, f, i, k, o** = 0.5 mm; **b–c, e, g–h, j** = 0.02 mm; **l–n, p** = 0.05 mm.

Table 2). Particularly, some primary spines (polypar and abpolypar spines) and secondary spines buttressed radially by 0–4 (mostly 2) inconspicuous, complete or incomplete, thin ridges are present in a specimen of extant *Stichopathes* spp. (Fig. 13j in ref. 39).

The only remaining concern challenging the antipatharian affinity of Sinopathidae¹⁰ is the presence of continuous fine longitudinal costellae in *Sinopathes reptans*. However, this fine sculpture is absent in extant black corals and specimens of Early Ordovician Fenxiang Formation identified as *Sinopathes* sp.¹². Longitudinal grooves and ridges (functioning as epidermal channels for water and nutrient transport)⁴⁰ are also common on the surface of multi-layered skeleton of octocorallians like *Corallium*, *Isidella*, and *Lepidisis*^{40–42}, but the size of these structures is up to about 200 times larger than that found on *Sinopathes*. The present morphological phylogenetic analyses suggest the updated Sinopathidae as a stem group of Antipatharia (Fig. 6a and Supplementary Fig. 6c), but whether the spine networks of Sterictopathidae originated from a common ancestor shared by Sinopathidae and Sterictopathidae remains unresolved.

Evolution of spine-ridge junctions in the black coral skeleton

The irregular arrangement of skeletal spines in the Early Ordovician black coral *Sinopathes reptans* was proposed to be a plesiomorphic trait, suggesting a subsequent evolutionary trend towards regularity^{11,12}. However, the previous evidence for this hypothesis is weak due to lacking of transitional fossils between Sinopathidae and extant black corals. Notably, *Sterictopathes radicans* from the same formation, which exhibits irregular skeletal networks, does not represent a transitional fossil species between Sinopathidae and extant families.

Instead, the present study identifies transitional black coral species (*Sterictopathes* sp., *Sterictopathes seira*) between the Early Ordovician

species *S. radicans* and extant black corals, allowing us to hypothesize some of the major evolution of skeleton regularity in black corals, as listed chronologically below: (1) The hypothesized ancestor of Sterictopathidae is assumed to have irregular networks with complete, uniformed, straight, and short ridges (Fig. 6f). (2) *S. radicans* from the Early Ordovician displays irregular networks with each spine buttressed mostly by 3–5 ridges (Fig. 6e). (3) *S. seira* from the Middle Ordovician exhibits degraded networks due to the vanishing tendency of transverse ridges, with each spine mainly comprising 2–3 ridges (Fig. 6d). (4) *Sterictopathes* sp. from the Middle Ordovician show simplified networks with almost complete disappearance of transverse ridges, with 0–2 ridges connecting each spine (Fig. 6c). (5) In modern black corals, networks are replaced either by isolated spines or spines connected by incomplete or complete, unnoticeable longitudinal ridges (Fig. 6b). The density of spines is lower in most modern black corals, which is probably due to more or less reduction of primary spines to secondary spines as seen in some extant forms, i.e., *Stichopathes* spp. (Fig. 13j in ref. 39), *Antipathes griggi* (Fig. 2e, f in ref. 43), *Antipathes fruticosa* (Fig. 9b, c in ref. 43), *Stichopathes* sp. SCBUCN-8850 (Fig. 3G–J in ref. 44). However, exceptions to this trend have been reported, including species such as *Cirrhopathes anguina*, *Cirrhopathes* cf. *indica*, *Cirrhopathes rumphii*, and *Stichopathes* cf. *maldivensis* (Figs. 14, 17, 19, 20, 23 in ref. 45). In summary, the number of spine-ridge junctions appears to decrease gradually from the Early Ordovician to modern black corals, and the arrangement of spines becomes more regular.

The rise and longitudinal fusion of networks

Due to lacking of soft-tissue preservation (i.e., polyps, mesenteries, and coenenchyme) in Ordovician black corals, the relationships between their soft-tissue and axial skeletons remain intriguing. We suggest that the deep

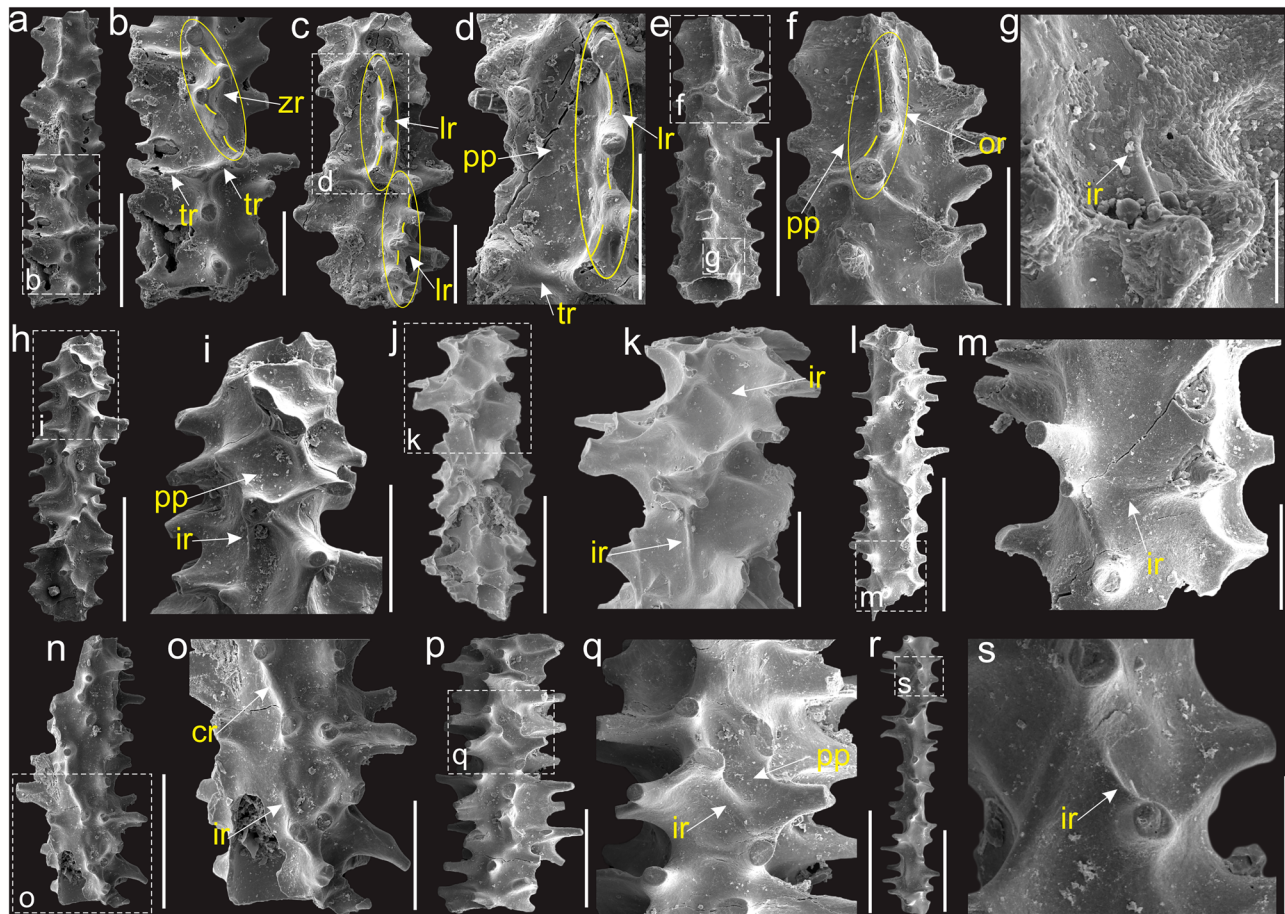


Fig. 4 | Networks formed by complete and incomplete ridges of *Sterictopathes seira* sp. nov. Abbreviations: CR complete ridge, IR incomplete ridge, LR long-itudinal subparallel rows of ridges, OR oblique ridge, PP polyp pit, TR transversal ridge, Zr zigzag row of ridges. Specimens: **a, b** ELI-FJG01293, **c, d** ELI-FJG01273, **e–g**

ELI-FJG02147, **h, i** ELI-FJG01089, **j, k** ELI-FJG03465, **l, m** ELI-FJG02398, **n, o** ELI-FJG02323, **p, q** ELI-FJG02189, **r, s** ELI-FJG02184. Scale bars, **a, e, h, j, l, n, p, r = 0.5 mm; b–d, f, i, k, o, q = 0.2 mm; g = 0.05 mm; m, s = 0.1 mm.**

network depressions in Sterictopathidae, although organic in composition, may find analogs in the polypoid pits or calcareous skeletal cups of colonial scleractinians, a group of colonial hexacorallians closely related to the Antipatharia⁴⁶. The bottom of the scleractinian cup, in widely spaced polyps, consists of a basal plate and a separate theca⁴⁷. But the scleractinian theca beneath tightly spaced polyps (i.e., *Favia*) appears as common walls, which are organized as polygonal networks⁴⁸ resembling that of Sterictopathidae.

Additionally, the fusion of skeletal cups into deep and long rows⁴⁸, seen in the derived clade of Hexacorallia (i.e., brain corals)⁴⁶, is highly reminiscent of the apparent trend of fusion and expansion of organic networks in Ordovician Sterictopathidae. In this regard, we infer that the deep network depressions and ridges in Sterictopathidae could be interpretable as polyp pits and organic theca walls, respectively. These networks may have facilitated the firm adherence of colonial polyps and ambient coenenchyme to the axial skeletal surface, preventing exfoliation by varying water currents on the continental shelf. Networks with abundant prominent spines, most likely, function effectively for defense (i.e., to prevent gnawing of predators). Furthermore, the occurrence of spines increases the surface area for cementing one skeletal layer to the other, while also acting as continuous rivets to resist delamination of shear forces produced by skeletal bending and torsion⁴⁹. If this statement is true, the occurrence of spines might eliminate or reduce the demand of small fibril biases between helically wound layers⁴⁹. The expansion of the network in Sterictopathidae, most probably, was advantageous in accommodating growing polyps and nutrient sharing among adjacent polyps. Particularly, the longitudinal fusion may relate to upward growth via asexual reproduction and rapid branch growth.

Origin of the antipatharian erect axial skeleton

The independent evolution of upright colonial forms⁴⁶ in Hydrozoa⁵⁰ and Octocorallia⁵¹, taken together with molecular phylogeny of anthozoans^{29,30,46}, may provide valuable hints into the rise of the upright axial skeleton of colonial antipatharians. The common ancestor of hexacorallians, likely soft-bodied and solitary in the Cryogenian–Ediacaran³⁰, may have secreted a basal, organic exoskeleton for fixing in/on the substrate (Fig. 6j). Against the backdrop of the Cambrian arms race and macrophagous predation^{52,53}, the asexual reproduction of polyps to increase body size (Fig. 6i) would lead to a sessile, sheet-like colony that may have independently arisen multiple times in different orders of cnidarians⁴⁶. Their sheet-like basal skeleton can be represented by the encrustation of *Sterictopathes radicans*¹² (Fig. 5p–u) and *S. seira* (Fig. 5m–o) on the tube wall of *Sphenothallus*.

The escalated ecological tiering competition among colonial, sessile suspension feeders in the Cambrian–Ordovician marine environments^{54,55} presumably have facilitated the independent evolution of upward growth of modular colonies, as exemplified by Sterictopathidae enclosing the *Sphenothallus* tube (Fig. 5m–u); their concentric axial skeleton (Fig. 6h) can be regarded as a stacking of annually secreted basal sheets, in microscope-scale deposition comparable to the calcareous lamellate skeleton of other fossil coral orders such as Tabulata and Rugosa⁵⁶.

Materials and Methods

Fossil and extant materials

In this study, 265 black corals fossils were examined (Supplementary Table 1). They were collected from the Middle Ordovician (Darrivillian Stage) Xiliangsi Formation at Fanjiagou section, Ningqiang county, Shaanxi,

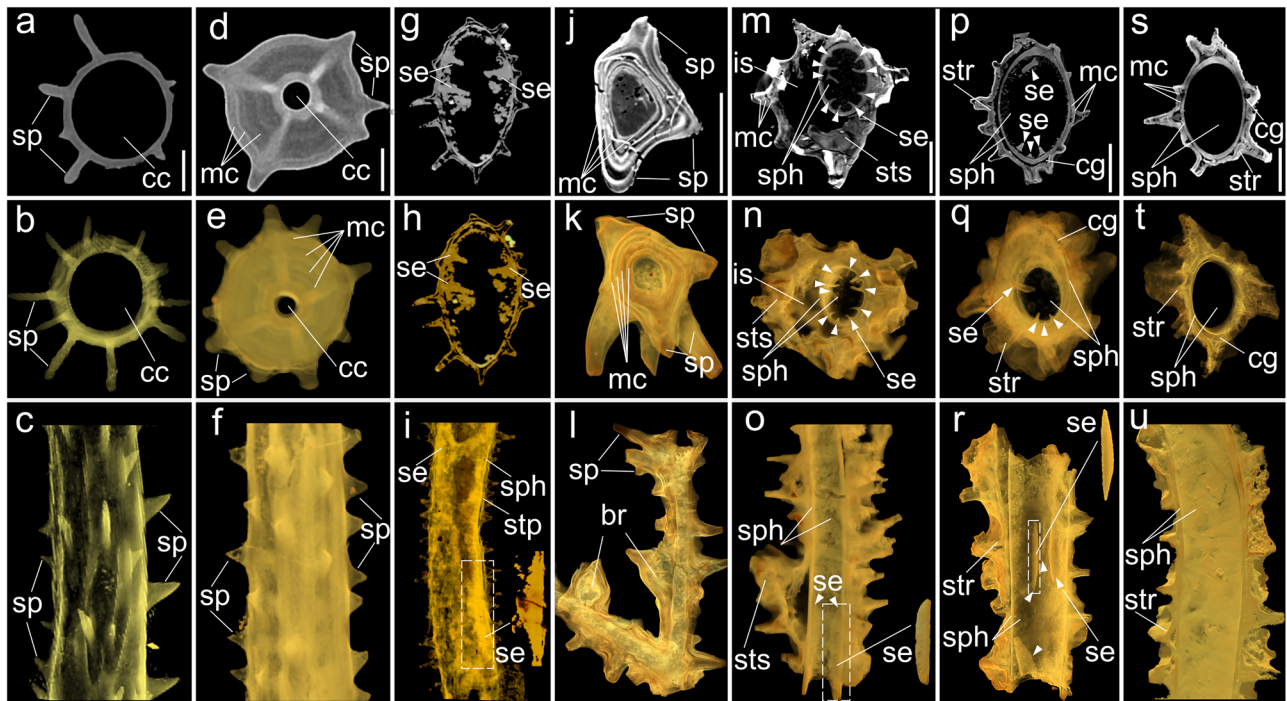


Fig. 5 | Morphological comparisons of extant and fossil black coral endoskeletons. **a–f** Extant black corals with characteristic internal multi-layered concentric structures. **a–c** Antipathidae, *Stichopathes spinosa*; **d–f** Antipathidae, *Antipathes sarothrum*. **g–u** Three fossil species of the family Sterictopathidae fam. nov.: **g–i** *Sterictopathes* sp. encrusting an interior tube of another Cnidaria *Sphenothallus* sp. with three characteristic internal septa (white arrows); **j–o** *Sterictopathes seira* sp. nov. with internal multi-layered concentric structure of itself (**j–l**) or encrusting the tube of *Sphenothallus* sp.; **m–o** with ten characteristic internal septa (white arrows); **p–u** *Sterictopathes radicans* encrusting two interior tubes of *Sphenothallus* sp., only

one tube (**p–r**) with four internal septa (white arrows). Specimens: **a–c** ZSM20030289, **d–f** ZSM20030284, **g–i** ELI-FJG04013, **j–l** ELI-FJG03118, **m–o** ELI-FJG02302, **p–r** ELI-HHC031, **s–u** ELI-HHC051. Abbreviations: BR branch, CG circular gap, CC central canal, IS irregular space, MC multi-layered concentric structure, RI ridge, SE septa, SP spine, SPH *Sphenothallus*, STP *Sterictopathes* sp., STR *Sterictopathes radicans*, STS *Sterictopathes seira*. Scale bars: **a–u** = 150 μm. The 3D construction data of the extant species *Leiopathes bullosa* (*Leiopathidae*) is available from Morphobank (accession number: M894365–M894377).

China (32°58'7.48"N, 106°28'7.99"E, specimen numbers with prefix ELI-FJG), and early Ordovician Fenxiang Formation in Huanghua quarry, Hubei, China (30°51'36.94"N, 111°21'49.64"E, with prefix ELI-HHC), respectively (Fig. 1). These fossils were recovered from limestone rocks through 5%–10% acetic acid leaching, and manually picked up from acid residues under a stereo microscope. The Middle Ordovician material from the Xiliangsi Formation comprised 253 specimens of *Sterictopathes seira* sp. nov. and three specimens provisionally identified as *Sterictopathes* sp. (Supplementary Table 1). Eight specimens of *S. radicans* were isolated from its type locality (Baliński & Sun, 2017) in the Fenxiang Formation, Hubei (Supplementary Table 1). All fossil specimens are deposited in Shaanxi Key Laboratory of Early Life and Environments, Northwest University, Xi'an, China.

For comparative analysis, type material of six extant species (*Antipathes sarothrum*, *Myriopathes stehowi*, *Stichopathes spinosa*, *Myriopathes bifaria*, *Leiopathes bullosa*, *Rhipidipathes colombiana*), deposited in Zoologische Staatssammlung München (prefix ZSM), was examined. Additionally, recent material of two black coral species (*Leiopathes* sp., *Leiopathidae*; *Tylopathes* sp., *Stylopathidae*) collected by the manned submersible *Shenhaiyongshi* from the South China Sea was utilized to observe internal compositions distributed between concentric skeleton layers. In situ and laboratorial images of the black coral *Bathypathes* sp. (*Schizopathidae*) collected by the manned submersible *Fendouzhe* from the Diamantina Fracture Zone was used for reference for artist reconstruction of the fossil species *Sterictopathes seira* sp. nov. The specimens collected by the submersibles are deposited in Institute of Deep-Sea Science and Engineering, Chinese Academy of Sciences (with prefix IDSSE).

Scanning electron microscopy

All investigated black coral specimens as well as other organisms in the Xiliangsi Formation, including trilobites, brachiopods, bivalve mollusks, pelagic conodonts, and index graptolites (Fig. 1, Supplementary Fig. 1) were imaged with a FEI Quanta 400 FEG scanning electron microscope (SEM).

X-ray tomographic microscopy

Sixteen selected fossil specimens and six extant black corals were scanned using microcomputed tomography (Micro-CT) (Xradia520 Versa) at Northwest University. Micro-CT 3D images and videos were segmented and visualized using VG studio 2.2 Max and Dragonfly 4.1 (Fig. 5).

Energy-dispersive X-ray spectrometry analyzes

Four specimens of *Sterictopathes seira* sp. nov. and *S. radicans* were analyzed under the environmental mode by Energy Dispersive X-ray spectrometry (EDS) system, with 20.0 kV, 60 Pa and WD 11.4 mm at Northwest University (Supplementary Fig. 4a–d).

Phylogenetic analysis

Three trees were generated by Bayesian inference-based phylogenetic analyzes: a morphological tree, a molecular tree, and a consensus tree combining morphological and molecular matrices (Supplementary Fig. 6; Supplementary Table 3, 4).

The morphological tree was constructed based on 26 characters extracted from 42 selected black coral species and the sea anemone outgroup *Nematostella vectensis* (Supplementary Fig. 6a, Supplementary Table 3, and Supplementary Date 1). The 36 extant black corals were selected from all eight extant black coral families. Priority was given to black coral species

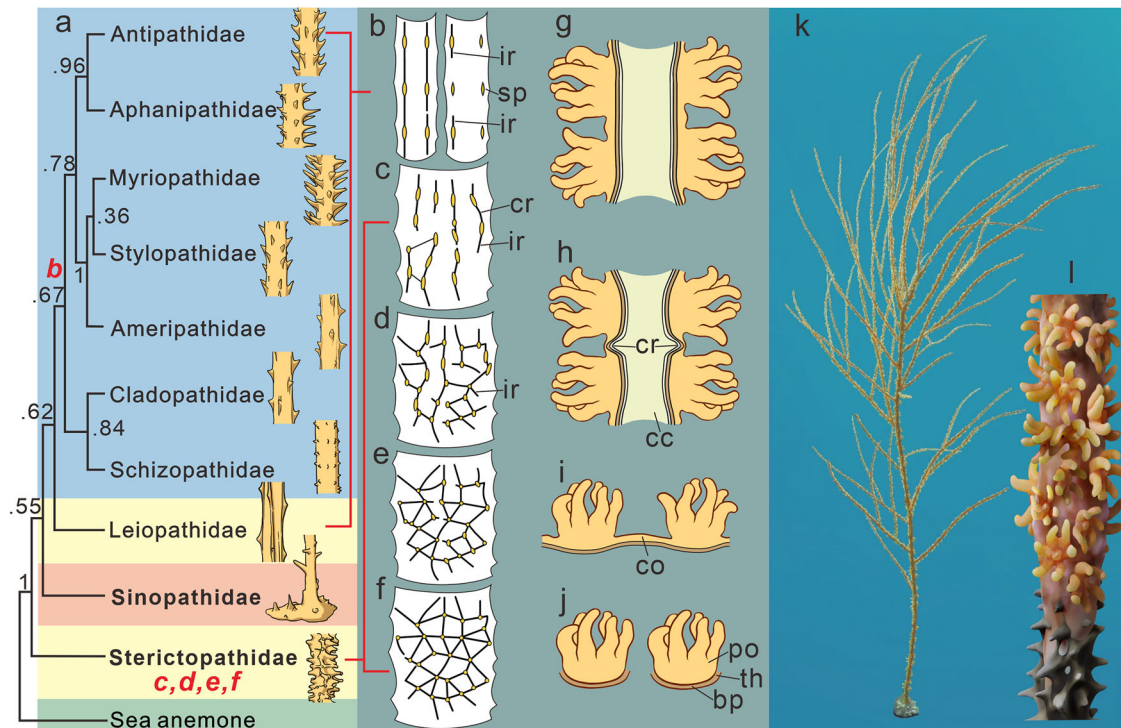


Fig. 6 | Evolution of skeleton regularity in black corals. **a** Bayesian analyzes concatenating morphology and molecular data for selected fossil and extant black corals (see detailed topology in Supplementary Fig. 6c); fossil families are shown in bold. **b** schematic construction of typical regular network types observed in eight extant black coral families. **c–e** Construction of irregular networks of three fossil species of the family Sterictopathidae fam. nov.: *Sterictopathes* sp. (c), *S. seira* (d) and *S. radicans* (e). **f** Conceptual ancestor of the Sterictopathidae fam. nov. with fully-developed irregular networks. **g–j** Hypothetical evolutionary trend of black coral

skeletal networks and ridges. Erected colonial black coral with (h) or without (g) ridges; i encrustation of ancestral colonial black corals by asexual reproduction; j ancestral solitary polypoid periderm of hexacorallian with a basal periderm. **k–l** Artist reconstructions of the black coral *Sterictopathes seira* sp. nov. Abbreviations: CO coenenchyme, BP basal plate, CC central canal, CR complete ridge, IR incomplete ridge, PO polyp, RI ridge, SP spine, TH theca.

with molecular data deposited in GenBank for analyzes. Morphological data were obtained from original species descriptions, recent re-descriptions (where available), specific fossil records, or extant specimens explicitly linked to published molecular data (Supplementary Table 3). Molecular data consisted of concatenated partial sequences of the COI, COIII, 18S and 28S genes (Supplementary Fig. 6b, Supplementary Table 4 and Supplementary Data 2). The consensus dataset combined the above morphological and molecular matrices (Supplementary Fig. 6c and Supplementary Data 3). Bayesian analyzes were run using MrBayes (v.3.2.7) and the GTR model, with gamma-distributed rate variation and variable coding. Bayesian analyzes were run using MrBayes (v.3.2.7) with data matrices and scripts detailed in Supplementary Data 1–3.

Raman spectroscopy

Raman spectra of *Sterictopathes seira* were obtained using a JY Horiba LabRam Odyssey equipped with a 532 nm laser source at Northwest University. Each target was subjected to a 30-second acquisition time with one accumulation, aiming to minimize laser-induced heating and achieve a favorable signal-to-noise ratio. The laser beam was directly focused on the fossil surface, and up to four distinct regions were probed for each sample. The Raman spectra were processed using LabSpec6 software (Supplementary Fig. 5e–h).

Comparative analysis of potential empty gaps in extant black coral skeleton layers

In this study, empty gaps were identified between fossil black coral skeleton layers. For comparative analysis, extant black corals were subjected to treatment with NaClO to eliminate proteins distributed between concentric skeleton layers. Branch pieces from *Leiopathes* sp. and *Tylopathes* sp.,

collected from the South China Sea, were immersed in 2 ml centrifuge tubes each containing 800 µl of sodium hypochlorite solution at 60 °C for 2 h. Subsequently, these samples were examined using micro-CT for 3D morphology (Supplementary Fig. 7) at Northwest University.

Reporting summary

Further information on research design is available in the Nature Portfolio Reporting Summary linked to this article.

Data availability

All original images and videos (3.42 G) that support this study have been deposited in Science Data Bank (DOI: 10.57760/sciencedb.12385) and MorphoBank (<https://morphobank.org/permalink/?P4854>).

Received: 5 June 2024; Accepted: 31 March 2025;

Published online: 07 April 2025

References

1. Agarwal, M. et al. Distribution and ecology of shallow-water black corals across a depth gradient on Galápagos rocky reefs. *Coral Reefs* **43**, 1–13 (2024).
2. Molodtsova, T. N. Black corals (Anthipatharia: Anthozoa: Cnidaria) of the north-eastern Atlantic. *Adv. Marine Biol.* **63**, 141–151 (2006).
3. Wagner, D. et al. The biology and ecology of black corals (Cnidaria: Anthozoa: Hexacorallia: Antipatharia). *Adv. Mar. Biol.* **63**, 67–132 (2012).
4. WoRMS. Antipatharia. Accessed at: <https://www.marinespecies.org/aphia.php?p=taxdetails&id=22549> (2024).

5. Cairns, S. Deep-water corals: an overview with special reference to diversity and distribution of deep-water Scleractinian corals. *Bull. Mar. Sci.* **81**, 311–322 (2007).
6. Bo, M. et al. *Antipatharians of the Mesophotic Zone: Four Case Studies. Mesophotic Coral Ecosystems*, Vol. 12 (Springer, 2019).
7. Molodtsova, T. N. et al. One of the deepest genera of Antipatharia: taxonomic position revealed and revised. *Diversity* **15**, 436 (2023).
8. Daly, M. et al. The phylum Cnidaria: A review of phylogenetic patterns and diversity 300 years after Linnaeus. *Zootaxa* **1668**, 127–182 (2007).
9. Horowitz, J. et al. Ameripathidae, a new family of antipatharian corals (Cnidaria, Anthozoa, Hexacorallia, Antipatharia). *ZooKeys* **1203**, 355 (2024).
10. Brugler, M., Opresko, D. & France, S. The evolutionary history of the order Antipatharia (Cnidaria: Anthozoa: Hexacorallia) as inferred from mitochondrial and nuclear DNA: implications for black coral taxonomy and systematics. *Zool. J. Linn. Soc.* **169**, 312–361 (2013).
11. Baliński, A., Sun, Y.-L. & Dzik, J. 470-Million-year-old black corals from China. *Naturwissenschaften* **99**, 645–653 (2012).
12. Baliński, A. & Sun, Y. -I. Early Ordovician black corals from China. *Bull. Geosci.* **92**, 1–12 (2017).
13. Michelin, H. *Iconographie Zoophytologique, Description Par Localités Et Terrains Des Polypiers Fossiles De France Et Pays Environnants* etc (Bertrand, 1840–1848).
14. Milne-Edwards, H. H. Monographie des Polypiers fossiles des terrains paléozoïques. *Archs Mus. Hist. nat. Paris* **5**, 1–502 (1851).
15. Wells J. W., H. D. Coelenterata. In: *Moore RC (ed) Treatise on Invertebrate Paleontology; part F. F1–F166* (Lawrence, 1956).
16. Michelotti, G. *Specimen Zoophytologiae Diluvianae* (Turin, 1839).
17. Kölliker, R. A. Die bindesubstanz der coelenteraten. *Icones histologicae oder Atlas der vergleichenden Gewebelehre.* **2**, 87–181 (1865).
18. Zittel, K. A. *Handbuch der Paläontologie. 1 Band. I Abtheilung Paläozoologie* (München, 1876–1880).
19. Pax, F. Beitrag zur Kenntnis der japanischen Dörnchenkorallen. *Zool* **63**, 407–450 (1932).
20. Edwards, H. M. & Haime, J. A monograph of the british fossil corals. First part. Introduction; Corals from the Tertiary and Cretaceous formations. *Palaeontogr* **3**, 1–71 (1850).
21. Horowitz, J. *The Taxonomy, Biodiversity, and Evolutionary History of Black Corals (Order Antipatharia)* PhD thesis, (James Cook University, 2022).
22. Bouillon, J. et al. *An Introduction to Hydrozoa* (Scientifiques du Muséum, 2006).
23. Opresko, D. M. Revision of the Antipatharia (Cnidaria: Anthozoa). Part II. Schizopathidae. *Zool. Med. Leiden.* **76**, 411–442 (2002).
24. Opresko, D. Revision of the Antipatharia (Cnidaria: Anthozoa). Part IV. Aphanipathidae. *Zool. Med. Leiden.* **78**, 209–240 (2004).
25. Opresko, D. Revision of the Antipatharia (Cnidaria: Anthozoa). Part III. Cladopathidae. *Zool. Med. Leiden.* **77**, 495–536 (2003).
26. Opresko, D. Revision of the Antipatharia (Cnidaria: Anthozoa). Part I. Establishment of a new family, Myriopathidae. *Zool. Med. Leiden.* **75**, 343–370 (2001).
27. Opresko, D. & Molodtsova, T. N. New species of deep-sea antipatharians from the North Pacific (Cnidaria: Anthozoa: Antipatharia), Part 2. *Zootaxa* **4999**, 401–422 (2021).
28. Chimienti et al. A new species of *Bathypathes* (Cnidaria, Anthozoa, Antipatharia, Schizopathidae) from the Red Sea and its phylogenetic position. *ZooKeys* **1116**, 1 (2022).
29. Horowitz, J. et al. Bathymetric evolution of black corals through deep time. *Proc. R. Soc. B* **290**, 20231107 (2023).
30. Quattrini, A. et al. Palaeoclimate ocean conditions shaped the evolution of corals and their skeletons through deep time. *Nat. Ecol. Evol.* **4**, 1531–1538 (2020).
31. Zhang, Y. et al. Ordovician integrative stratigraphy and timescale of China. *Sci. China Earth Sci.* **62**, 61–88 (2019).
32. Lai, C. G. et al. Restudy of the Ordovician of southern Shaanxi-northern Sichuan Areas. *Profess. Pap. Stratigr. Palaeontol.* **23**, 1–36 (1990).
33. Feng, Z. *Lithofacies Paleogeography of the Cambrian and Ordovician in South China* (Geological Publishing House, 2004).
34. Balinski, A. & Sun, Y. Fenxiang biota: a new Early Ordovician shallow-water fauna with soft-part preservation from China. *Sci. Bull.* **60**, 812–818 (2015).
35. Goldberg, W. Chemistry and structure of skeletal growth rings in the black coral *Antipathes fiordensis* (Cnidaria, Antipatharia). *Hydrobiologia* **216**, 403–409 (1991).
36. Dzik, J., Baliński, A. & Sun, Y.-L. The origin of tetra-radial symmetry in cnidarians. *Lethaia.* **50**, 306–321 (2017).
37. Bengtson, S. Early Cambrian fossils from South Australia. *Mem. Assoc. Australas. Palaeontol.* **9**, 1–364 (1990).
38. Barrett, N. et al. Phylogenetics and mitogenome organisation in black corals (Anthozoa: Hexacorallia: Antipatharia): an order-wide survey inferred from complete mitochondrial genomes. *Front. Mar. Sci.* **7**, 440 (2020).
39. Terrana, L. et al. Whip black corals (Antipatharia: Antipathidae: *Stichopathes*) of the Mesophotic Coral Ecosystem of Mo’orea (French Polynesia), with the description of a new species. *Zootaxa* **5486**, 182–212 (2024).
40. Grillo, M. C., Goldberg, W. M. & Allemand, D. Skeleton and sclerite formation in the precious red coral *Corallium rubrum*. *Mar. Biol.* **117**, 119–128 (1993).
41. Tu, T.-H., Dai, C.-F. & Jeng, M.-S. Taxonomic revision of Coralliidae with descriptions of new species from New Caledonia and the Hawaiian Archipelago. *Mar. Biol. Res.* **12**, 1003–1038 (2016).
42. Goedert, J., Guthrie, L. & Kiel, S. Octocorals (Alcyonacea and Pennatulacea) from Paleogene deep-water strata in western Washington State, USA. *J. Paleontol.* **96**, 539–551 (2022).
43. Opresko, D. A new name for the Hawaiian antipatharian coral formerly known as *Antipathes dichotoma* (Cnidaria: Anthozoa: Antipatharia) 1. *Pac. Sci.* **63**, 277–291 (2009).
44. Tapia-Guerra, J. et al. First ecological characterization of whip black coral assemblages (Hexacorallia: Antipatharia) in the Easter Island Ecoregion, Southeastern Pacific. *Front. Mar. Sci.* **8**, 755898 (2021).
45. Terrana, L., Bo, M., Opresko, D. M. & Eeckhaut, I. Shallow-water black corals (Cnidaria: Anthozoa: Hexacorallia: Antipatharia) from SW Madagascar. *Zootaxa* **4826**, 1–62 (2020).
46. McFadden, C. et al. Phylogenomics, Origin and Diversification of Anthozoans (Phylum Cnidaria). *Syst. Biol.* **70**, 635–647 (2021).
47. Hyman, L. H. *The Invertebrates: Protozoa through Ctenophora* (Libbie Henrietta, 1940).
48. Ruppert, E. E., Fox, R. S. & Barnes, R. D. *Invertebrate Zoology: A Functional Evolutionary Approach* (Thomson-Brooks/Cole, 2004).
49. Kim, K., Goldberg, W. M. & Taylor, G. T. Architectural and mechanical properties of the black coral skeleton (Coelenterata: Antipatharia): a comparison of two species. *Biol. Bull.* **182**, 195–209 (1992).
50. Cartwright, P. The development and evolution of hydrozoan polyp and colony form. *Hydrobiologia* **530**, 309–317 (2004).
51. Fretter, V. & Graham, A. *A Functional Anatomy of Invertebrates* (Academic Press, 1976).
52. Ou, Q. et al. Dawn of complex animal food webs: a new predatory anthozoan (Cnidaria) from Cambrian. *The Innovation.* **3**, 1 (2022).
53. Bengtson, S. Origins and early evolution of predation. *Paleontol. Soc. Pap.* **8**, 289–318 (2002).
54. Ausich, W. I. & Bottjer, D. J. Tiering in suspension-feeding communities on soft substrata throughout the Phanerozoic. *Science* **216**, 173–174 (1982).
55. Bottjer, D. J. & Ausich, W. I. Phanerozoic development of tiering in soft substrata suspension-feeding communities. *Paleobiology* **12**, 400–420 (1986).

56. Wendt, J. Corals and coralline sponges. *Skeletal Biomineralization: Patterns, Processes and Evolutionary Trends* (ed Joseph G. Carter) 5, 45–66 (Springer, 1989).

Acknowledgements

We thank Prof. Yuanlin Sun (Peking University) for insightful suggestions on field work, the assistance of all onboard staffs during the deep-sea cruises conducted by the R/Vs *Tansuoyihao* and *Tanshuoerhao* (IDSSE). We also thank Jingpeng Yuan for the artistic reconstructions, Hujun Gong, Juan Luo, and Na Liu (Northwest University) for their assistance with laboratory work, Prof. Glen Brock (Macquarie University), Kun Liang (Nanjing Institute of Geology and Palaeontology, CAS), Xiuchun Jing (China University of Geosciences, Beijing) and Qiang Ou (China University of Geosciences, Beijing) for discussions of the earlier draft, Lucas Terrana (Université Libre de Bruxelles) and two anonymous reviewers for their significant comments. This study was supported by the National Key Research and Development Program of China (2023YFF0803601), the National Natural Science Foundation of China (42372012, 42276090, 41720104002, 42202009), the International Partnership Program of Chinese Academy of Sciences (183446KYSB20210002), the project of IDSSE, Chinese Academy of Sciences (E371020101), Hainan Provincial Natural Science Foundation of China (324MS114), and the Programme of Introducing Talents of Discipline to Universities (D17013).

Author contributions

J.H. and X.S. designed and organized the research, provided research funding; J.H., X.S., W.H., A.B., M.B., Y.Y., and T.K. wrote the paper; J.H., W.H., D.W., X.W., and Y.Y. collected the fossil material; W.H., J.H., and X.W. examined the fossil material; X.S., M.R.B. and B.R. examined the extant materials; W.H., J.H., X.S., and A.B. prepared the systematics; X.S., W.H., and D.W. ran the phylogenetic analyses; J.S., W.H., T.K., and Y.Y. performed micro-CT 3D constructions. All authors revised the manuscript.

Competing interests

The authors declare no competing interests.

Additional information

Supplementary information The online version contains supplementary material available at <https://doi.org/10.1038/s42003-025-08022-x>.

Correspondence and requests for materials should be addressed to Jian Han or Xikun Song.

Peer review information *Communications Biology* thanks Lucas Terrana and the other, anonymous, reviewer(s) for their contribution to the peer review of this work. Primary Handling Editors: Aylin Bircan, Ophelia Bu.

Reprints and permissions information is available at <http://www.nature.com/reprints>

Publisher's note Springer Nature remains neutral with regard to jurisdictional claims in published maps and institutional affiliations.

Open Access This article is licensed under a Creative Commons Attribution-NonCommercial-NoDerivatives 4.0 International License, which permits any non-commercial use, sharing, distribution and reproduction in any medium or format, as long as you give appropriate credit to the original author(s) and the source, provide a link to the Creative Commons licence, and indicate if you modified the licensed material. You do not have permission under this licence to share adapted material derived from this article or parts of it. The images or other third party material in this article are included in the article's Creative Commons licence, unless indicated otherwise in a credit line to the material. If material is not included in the article's Creative Commons licence and your intended use is not permitted by statutory regulation or exceeds the permitted use, you will need to obtain permission directly from the copyright holder. To view a copy of this licence, visit <http://creativecommons.org/licenses/by-nc-nd/4.0/>.

© The Author(s) 2025